Atmospheric Environment 301 (2023) 119670

Contents lists available at ScienceDirect

Atmospheric Environment

journal homepage: www.elsevier.com/locate/atmosenv

Fine micro- and nanoplastics particles ($PM_{2.5}$) in urban air and their relation to polycyclic aromatic hydrocarbons

Bernadette Kirchsteiger [a,1], Dušan Materić [b,c,*,1], Felix Happenhofer [a], Rupert Holzinger [b], Anne Kasper-Giebl [a]

[a] Institute of Chemical Technologies and Analytics, TU Wien, Getreidemarkt 9, A-1060, Vienna, Austria
[b] Institute of Marine and Atmospheric Research Utrecht, Utrecht University, Princetonplein 5, 3584CC, Utrecht, the Netherlands
[c] Department for Analytical Chemistry, Helmholtz Centre for Environmental Research – UFZ, Permoserstraße 15, 04318, Leipzig, Germany

HIGHLIGHTS

- We measured atmospheric concentrations of three polymer types in urban $PM_{2.5}$ samples.
- Mean plastic concentration (size <2.5 μm) was 238 ng/m^3, which is 0.67% of $PM_{2.5}$ mass.
- Correlations of PP and PE with single PAH congeners were identified.
- Correlations are more likely with low molecular weight PAHs and polymers.
- Results indicate possible PAH carrier activities of UFMNP.

GRAPHICAL ABSTRACT

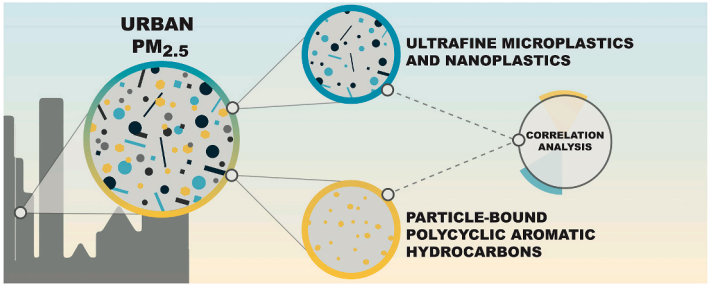

ARTICLE INFO

Keywords:
Ambient $PM_{2.5}$
Ultrafine microplastic and nanoplastics
Polycyclic aromatic hydrocarbons
Vehicles for atmospheric transport
Emerging pollutants

ABSTRACT

Microplastics and nanoplastics have been reported in nearly all environmental compartments, the dataset about their contributions and their role as a sink and carrier for other hydrophobic compounds in the atmosphere however is limited. This study presents, for the first time, atmospheric concentrations of ultrafine microplastics and nanoplastics (UFMNP) on the single polymer level and their correlations with atmospheric concentrations of 23 polycyclic aromatic hydrocarbons (PAHs). Measurements of UFMNP in ambient particulate matter ($PM_{2.5}$) were performed for an urban sampling site in Graz, Austria. During the sampling period of 02.01. – 31.03.2017 the average UFMNP concentration was 238 ng/m^3, reaching up to 557 ng/m^3. This accounts for an average contribution of 0.67% to $PM_{2.5}$ mass and 1.7% of organic matter. The individual polymer types were polyethylene terephthalate (PET), polypropylene (PP) and polyethylene (PE), which sum up the most demanded polymer types in Europe. PET was found to be the most prominent polymer in the urban samples contributing to 50% of the overall UFMNP mass, followed by PP (27%) and PE (23%). However, the relative contributions vary with time. PET was observed during the entire time period, while PP and PE were quite variable and linked to the origin of the air masses. A possible carrier function of PP and PE for selected micropollutants can be deduced from the significant monotonic correlations between these polymers and selected PAHs. High correlations were predominantly found for low molecular weight congeners and correlations were more pronounced than those investigated for PAHs and other constituents of $PM_{2.5}$, i.e. elemental carbon and organic matter again pointing to special interactions of those emerging pollutants.

* Corresponding author. Institute of Marine and Atmospheric Research Utrecht, Utrecht University, Princetonplein 5, 3584CC, Utrecht, the Netherlands.
E-mail address: d.materic@uu.nl (D. Materić).
[1] Contributed equally.

https://doi.org/10.1016/j.atmosenv.2023.119670
Received 11 November 2022; Received in revised form 3 February 2023; Accepted 19 February 2023
Available online 28 February 2023

1. Introduction

Plastic compounds define our way of living. To satisfy the society's needs, plastic production has drastically risen over the past years, and in 2020, 367 million tons of plastics were produced worldwide, whereas 55 million tons were produced in Europe (Plastics Europe, 2021). Plastic compounds usually have a life time up to 50 years, and then undergo post lifetime processing such as being disposed in landfills, used for energy production or being recycled. Although recycling of plastic compounds is favored, only 34.6% of 29.5 million tons collected plastic waste has been recycled in 2020 (Plastics Europe, 2021). Mismanaged macro plastic waste (>5 mm) enters the environment leading to degradation of plastic compounds yielding micro- and nano-sized fractions as a consequence of being exposed to different environments (Gasperi et al., 2018). In recent years, two particular size fractions of plastic compounds gained emerging focus: (i) microplastics (MPs) comprising plastic particles with 1 μm–5 mm in size and (ii) nanoplastics comprising plastic particles smaller than 1 μm in size (Allen et al., 2022). To date, MPs have been reported in nearly all environmental compartments. Most of them referring to the aquatic systems, e.g. oceans (e.g. Avio et al., 2017; Hirai et al., 2011), riverine systems (e.g. Mai et al., 2020), lakes and surface waters (e.g. Materić et al., 2022b), soil and sediments (e.g. Corradini et al., 2019). Knowledge about MPs as air pollutants is scarce (Sridharan et al., 2021), still MPs were identified in ambient aerosols and atmospheric deposition in (sub-)urban environments (e.g. Cai et al., 2017; Dris et al., 2016; Klein and Fischer, 2019; Wright et al., 2020). The identification of MPs in remote areas further indicates their possibility of atmospheric transport (e.g. Allen et al., 2019; Bergmann et al., 2022; Materić et al., 2022a; Materić et al., 2021).

Besides identifying MPs in different environmental matrices, their interaction with co-occurring pollutants enhances concern. It is well known, that MPs have the ability to adsorb organic pollutants like polycyclic aromatic hydrocarbons (PAHs) (Torres et al., 2021; Wang et al., 2020), which pose an even higher environmental and toxicological threat. PAH concentrations adsorbed to MPs have been found to exceed the PAH concentrations found in the respective aquatic phase by several orders of magnitude (Rochman et al., 2013). The important parameters of polymer types influencing the sorption/desorption mechanism of organic pollutants are: specific surface area, particle size, crystallinity, degree of cross-linking and spatial arrangement of the polymer itself (Wang et al., 2020). The interaction between pollutants will also be modified by other transformation mechanism like the photooxidation and abrasion of MPs, which leads to a loss of mechanical integrity and stability as well as changes in the chemical behavior (Fotopoulou et al., 2015). Consequently different polymer types have different sorption abilities of organic pollutants. Most sorption experiments are carried out under well-defined lab-conditions (e.g. Lee et al., 2014; Seidensticker et al., 2017; Wang and Wang, 2018), while only a limited number of works refers to sorption experiments of organic pollutants to MPs realized within field-measurements (Rochman et al., 2013). Even tough, adverse health effects may increase as MPs tend to carry other pollutants from its surroundings (Gasperi et al., 2018), literature discussing the co-occurrence of MPs and other associated substances an ambient air is scarce. A first indication describing the connection of MPs and PAHs in ambient air was given by Akhbarizadeh et al. (2021), clearly highlighting the growing need of these kind of studies.

With this work, we aim (1) to quantify atmospheric concentrations of ultrafine microplastics and nanoplastics <2.5 μm in aerodynamic diameter (UFMNP) and 23 individual PAH congeners at an urban sampling site and to (2) investigate the respective mass contributions to aerosol mass as well as correlations between the polymers and PAHs as examples of toxic micropollutants to identify possible carrier activities.

2. Material and methods

2.1. Sampling location and sample collection

$PM_{2.5}$ (particles up to a size of 2.5 μm aerodynamic diameter) sampling was done at an urban sampling station in Graz Don Bosco (GDB) (LON 15.41643°, LAT 47.05702°, ALT 358 m) located nearby a densely trafficked crossway in the north-western part of the city. Samples were collected within the Styrian air quality network on quartz fibre filters (Pall Life Sciences) according to the reference method for PM sampling using a Digitel high volume sampler (flow rate: 30 m^3/h, sampling duration: 24 h). $PM_{2.5}$ mass was gravimetrically determined according to DIN EN 12341:2014 (EN 12341, 2014). From the time period of 02.01.2017 to 31.03.2017, 29 daily samples were selected for chemical analyses, with most samples (n = 19) selected before 02.02.2017 and five other samples selected for each, February and March. The time period of interest is quite special as during that time high PM burdens were reported across mid-Europe and thus also in Graz (EEA, 2019).

For additional data evaluation PM_{10} concentrations were determined at GDB and at Bockberg (BB). BB is not directly influenced by urban emissions and thus represents a background sampling site (LON 15.49583°, LAT 4687139°, ALT 449 m). PM_{10} concentrations at BB were sampled with a beta attenuation mass monitor (MetOne BAM 1020, flow rate: 1 m^3/h, EN 16450:2017 (EN 16450, 2017)) while an additional Digitel high volume sampler was operated at GDB.

2.2. Sample selection and classification

To further explore the relationship between polymer and PM concentrations as well as possible sources, we utilize an approach based on the concept of the urban impact (Lenschow et al., 2001). This rather simple approach was used to have a first approximation to differentiate between local and regional sources during a period of high PM concentrations as explained in the prior section. Based on PM_{10} concentrations determined at GDB and the background site Bockberg (BB), Kirchsteiger et al. (2020) identified time periods affected by long range transport (i.e. days showing quite similar concentration between GDB and BB and mass ratios ≤1.5) and days dominated by an influence of local sources (mass ratio >2). Applying this approach to the data investigated here the sub-groups 'local' and 'regional' consisting of 10 samples each are defined. 9 samples are summarized in the sub-group 'unassigned' (mass ratio between 1.5 and 2). Samples of the ‚unassigned' group comprise samples which could neither be classified as being mainly of local origin or mainly affected by regional transport. This study focusses on days differing in PM_{10} ratios and thus effected by different source contributions. Samples assigned to the respective classes are highlighted in Fig. 1 and further details about the PM masses and ratios are given in the supplement. Chemical analysis was performed using $PM_{2.5}$ samples, as PM_{10} data was only available from online monitoring and not for off-line chemical investigation.

2.3. TD-PTR-MS

Ultrafine microplastics and nanoplastics <2.5 μm aerodynamic diameter (UFMNP), was quantified using PTR-MS 8000 (IONICON Analytik, Austria) equipped with a thermal desorption (TD) unit. For that filter punches (5 mm diameter) were transferred to a prebaked glass vial (overnight at 250 °C) and loaded into the TD oven. The thermal desorption sequence (35 °C for 3 min, ramp to 350 °C at rate of 40 °C/min and hold time for 4 min at 360 °C) was started subsequently. Components were transferred to the PTR-MS instrument in a clean carrier gas stream (N_2 5.0, flow: 50 ml/min). PTR-MS measurements were realized at an acquisition rate of 1 s with an E/N of 120 Td and mass spectra covered a m/z range up to 457 Da.

In terms, of quality assurance we conducted additional measurements, i.e. samples and blanks spiked with polystyrene microplastics (1

μm diameter). For that we used a similar setup also equipped with a TD unit, but a PTR-MS 4000 (IONICON Analytik, Austria). In total, we analysed 29 samples (in duplicates) and 7 field blanks using the same protocol.

Raw data was processed using PTRwid (Holzinger, 2015) which includes the peak integration and extraction and average and merging of raw mass spectra. When the temperature in the thermal desorption setup reached 50 °C 10 min peak integration was started, which yields an average mass spectrum for each TD run. The resulting ion signals were corrected using the ion signals obtained during field blank measurements and the respective detection limit (LOD). LODs refer to three times the standard deviation of the ion signals of all system blank signals (n = 9). The final mass spectra were used for nanoplastics fingerprinting, which has been described previously by Materić et al., 2020, 2021, 2022b.

2.4. Particle-bound PAHs

The quantitative analysis of 23 PAHs was performed according to EN 15549:2008–06 (EN 15549, 2008) using a dichloromethane and cyclohexane mixture (1/1, v/v) for ultrasonic extraction. Samples were analysed using a gas chromatograph (GC) system (Hewlett Packard, HP 6890) coupled to a mass spectrometer (MS) (Agilent, MS 5973) with an electron ionization (EI) source. Separation was achieved using a Zebron ZB5MSplus, non-polar and high temperature stable capillary column (30 m × 0.25 mm x 0.25 μm). More details about the analytical procedure and method parameters are given in the supplement.

PAH quantification was performed for 26 samples (in duplicates). Furthermore 1,3,5-triphenylbenzene (135TPB), a tracer substance for PE combustion processes, was analysed. Quantified PAHs were the following: acenaphthylene (Acy), acenaphthene (Ace), fluorene (Fluo), phenanthrene (Phen), anthracene (Anthr), fluoranthene (Fla), pyrene (Pyr), benz[*a*]anthracene (BaA), chrysene (Chry), benzo[*a*]fluoranthene (BaF), benzo[*b*]fluoranthene (BbF), benzo[*k*]fluoranthene (BkF), benzo[*j*]fluoranthene (BjF), benzo[*e*]pyrene (BeP), benzo[*a*]pyrene (BaP), perylene (Per), indeno[*1,2,3-cd*]pyrene (IcdP), dibenz[*a,h*]anthracene (DBahA), benzo[*ghi*]perylene (BghiP), dibenzo[*a,e*]pyrene (DBaeP), dibenzo[*a,i*]pyrene (DBaiP), dibenzo[*a,l*]pyrene (DBalP) and coronene (Cor). The three benzofluoranthenes isomers, i.e. BbF, BkF and BjF were quantified as sum and thus abbreviated as BbjkF in the following. A more detailed information about the quantified PAHs is given in the supplement (Table S1).

2.5. OC/EC

Carbonaceous compounds, i.e. organic carbon (OC) and elemental carbon (EC) were determined by thermal-optical analysis, using and OCEC Analyzer (Sunset Laboratory Inc.) from filter aliquots with a diameter of 10 mm. Analysis was done according to EN 16909:2017–06 (EN 16909, 2017) using the EUSAAR2 protocol (Cavalli et al., 2010). All measurements were done in duplicates. To derive organic matter (OM) a conversion factor of 1.5 was applied (OM = 1.5*OC) (Kirchsteiger et al., 2020).

2.6. Statistical data evaluation

Differences among the assigned classes, i.e. local, regional and unassigned, were evaluated based on one-way ANOVA. Investigation of possible relationships among polymer types and macro- and micro constituents of PM was realized using Spearman rank analysis based on the whole dataset, i.e. including all available data points no matter of classification. All statistical analysis was performed using the statistical software R (Version 3.6.3).

2.7. Quality assurance

For ultrafine microplastics and nanoplastics <2.5 μm aerodynamic diameter (UFMNP), to assess possible contamination due to sample handling or the analytical procedure, system blanks (clean vial, n = 9) and field blanks (n = 7) were analysed. The field blanks were exposed to the same environmental influencing factors and surroundings as PM samples. Although samples and blanks were stored in PE bags, we found PE fingerprints in only 4 of the field blanks, resulting in a mean PE concentration of 9.7 ± 10.0 ng/run. For the comparison, when PE quantities are detected in the samples we measured on average 97.0 ng/run (ranging 5.9–235 ng/run). Furthermore, 6 field blanks matched positive for both, PET and PP fingerprints. The levels of the field blanks PET and PP contamination were 5.3 ± 3.6 ng/run and 10.6 ± 3.9 ng/run, respectively. In the comparison, the average PET and PP levels when detected in the samples were 124 (ranging 9.0–218) and 96.6 (ranging 6.8–273) ng/run. We corrected the final concertation values of the samples by the blank subtraction also applying the strict 3-sigma detection limit filter as presented in Materić et al. (2020).

To assess the possible matrix effect to the micro/nanoplastics detection by TD-PTR-MS we performed an experiment where we spiked the samples and blanks with 200 ng of polystyrene spheres (1 μm in diameter). Both blanks and samples showed a clear fingerprint match for polystyrene (given in the supplementary data repository).

For PAHs, field blanks (n = 4) were analysed using the same setup and sample preparation procedure as described above. Blanks did not show quantifiable concentrations of any PAH congener, indicating that sample contamination due to the sampling and sample preparation procedure can be neglected. The same procedure was applied to a certified reference material (ERM CZ-100®, PM_{10}-like) in terms of quality control. The average recovery rate of BaP obtained for reference measurements was 105% (n = 4).

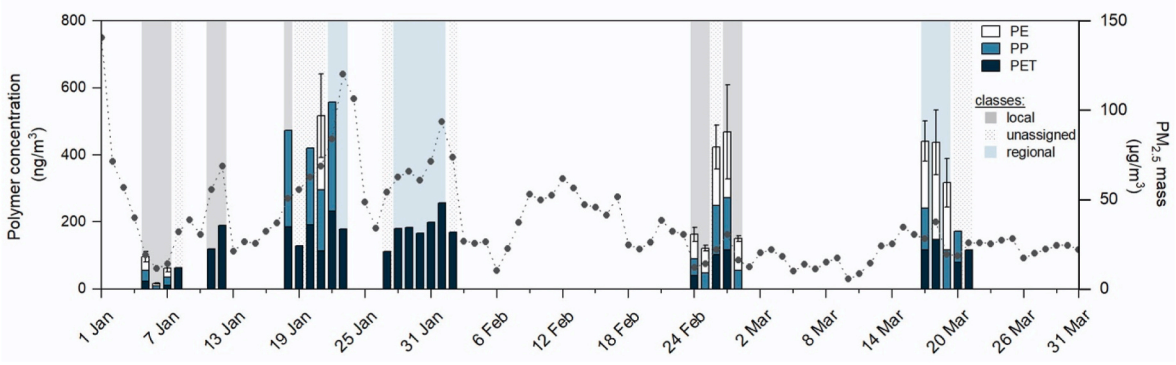

Fig. 1. Atmospheric UFMNP and $PM_{2.5}$ concentrations observed throughout the sampling period. Error bars at UFMNP concentration represent the measurement uncertainty of ±30%. Samples assigned to the respective classes are highlighted as noted in the graph.

For OC and EC, also field blanks (n = 7) were analysed and came up to a value of 2.28 μg/cm^2 for OC while no EC was detected on the blanks.

3. Results and discussion

3.1. Ultrafine microplastics and nanoplastics in urban samples

UFMNP averaged at 238 ng/m^3 (ranging from 16.7 to 557 ng/m^3) (n = 29). The average mass contribution of UFMNP to $PM_{2.5}$ is 0.67%, with maximum contributions of 1.9%, while the average contributions of OM and EC was 38% and 5.7%, respectively. The remaining $PM_{2.5}$ mass, which is not explicitly mentioned here, was mainly inorganic ions and mineral dust. A detailed chemical evaluation and source apportionment of samples representing this time period is presented elsewhere (Kirchsteiger et al., 2020). Focusing on organics, the contribution of UFMNP to OM reaches an average value of 1.7% and a maximum value of 4.5%. A timeline of measured UFMNP sub grouped in the individual polymer types is given in Fig. 1. A list of atmospheric concentrations of all key components discussed in this study is given in the supplement (Table S 2). In contrast to $PM_{2.5}$ mass, UFMNP concentrations did not show a declining trend from January to March (see Fig. 1). Peak UFMNP concentrations occurred during the time period of 18.01. – 23.01. 2017, but also in February and March. High UFMNP concentrations observed during the first time period, i.e. 18.01. – 22.01.2017, were accompanied by rather high $PM_{2.5}$ concentrations (50.7–83.9 μg/m^3), while this was not the case for the samples from late February and March ($PM_{2.5}$ mass: 22.1–37.6 μg/m^3). Interestingly UFMNP concentrations determined from 23.01. – 02.02.2017 were rather low, although $PM_{2.5}$ reach even higher values than in the preceding period of 18.01.-22.02.2017. We will come back to this phenomenon later, when single polymer types are discussed. Lowest UFMNP concentrations could be observed on the 06.01.2017 with 16.7 ng/m^3, when overall $PM_{2.5}$ was also a minimum (11.4 μg/m^3).

Different detected polymer types refer to polyethylene terephthalate (PET), polypropylene (PP) and polyethylene (PE), which are among the most demanded polymer types in Europe and mainly used for packaging, building and construction purposes (Plastics Europe, 2021). The occurrence of these three types of polymers agrees with data reported previously from cities in France and China (Cai et al., 2017; Dris et al., 2016) or for background environments (Allen et al., 2022), which all report important contributions of PET, PP and PE in deposited nano to microplastics. We did not find other emerging polymer types such as polystyrene or polyvinyl carbonate in our samples. However, relative contributions of different polymer types observed in atmospheric deposition samples vary within a yearly timeline (Allen et al., 2022).

PET was found to be the most prominent polymer in the urban $PM_{2.5}$ samples. It was found in the majority of samples (n = 25), contributing on average 50% to the overall UFMNP mass. The atmospheric concentrations of PET ranged from 10.6 to 256 ng/m^3. In 2020, PET demand in Europe was more than 4 million tonnes which accounts for 8.4% of all polymer types used (Plastics Europe, 2021).

The number of matches for PP and PE in the urban $PM_{2.5}$ samples was lower, although PP and PE are the top two demanded polymer types in Europe, with demands of more than 14 and 9 million tonnes, respectively (Plastics Europe, 2021). Considering these two polymer types, PP was found in a larger number of samples (n = 16) than PE (n = 12) with relative contributions accounting for 27% (PP) and 23% (PE) of the overall UFMNP mass. The atmospheric concentrations of PP were in the range of 8.49–326 ng/m^3, while slightly lower ones were observed for PE, ranging from 8.16 to 290 ng/m^3 (n = 12).

Polymer patterns seem to change with proceeding time indicating that also source impacts or transport and transformation processes within the atmosphere change. Changes are particularly evident at the end of January, when only PET was identified, although $PM_{2.5}$ concentrations were rather high. Starting on 20.01.2017 and lasting end of January a winter episode of high pollution occurred across Europe, accompanied with long-range transport of PM (EEA, 2019). Samples derived later, i.e. during February and March show a more diverse contribution of polymer types and PP and PE becoming more abundant than PET. We cannot give a reason for these differences in polymer patterns currently, but there is evidence that this effect was visible at a larger scale. Materić et al. (2021) analysed nanoplastics deposited onto the snow cover at a remote site in the Austrian Alps (Sonnblick Observatory). The observation time covered 06.02. −20.03.2017 and thus the second half of the measurements presented here. Only PET was determined until 25.02.2017, while later samples showed PP concentrations being more dominant (Materić et al., 2021). This PET dominated period, of which we unfortunately do not have any samples, directly follows the PET dominated period reported here. Still another high pollution episode is reported from 09.02.-17.02.2017 (EEA, 2019).

3.2. Differences of $PM_{2.5}$ and polymer concentrations between assigned classes

Fig. 2 A presents the atmospheric $PM_{2.5}$ concentrations grouped according to the three different classes, i.e. local, unassigned and regional. $PM_{2.5}$ concentrations of the regional class were higher (median: 64.1 μg/m^3) than the ones observed for samples of the local (median: 17.6 μg/m^3) and unassigned class (median: 54.2 μg/m^3). Statistical evaluation based on one-way ANOVA proved this impression and identified a significant difference among those classes (F-value = 4.949, p-value = 0.0151).

Fig. 2 B presents the boxplots of atmospheric PET concentrations for the local, unassigned and regional data sets, yielding median concentrations of 31.5 ng/m^3, 113 ng/m^3 and 180 ng/m^3, respectively. One-way ANOVA showed a significant difference of atmospheric PET concentrations between the assigned classes (F-value = 4.565, p-value = 0.0204). Median concentrations followed the trend of the overall picture of $PM_{2.5}$. Obviously PET concentrations correspond with $PM_{2.5}$ concentrations and a separation between days influenced stronger by transport or local emissions is of minor importance.

In case of the other two quantified polymer types, the patterns were quite different. PP (see Fig. 2 C) was found in most of the samples assigned to the local class (n = 8), yielding median concentrations of 40.5 ng/m^3 (local). Still, several samples of the other classes missed PP. Consequently, variability get huge and concentrations reach from not detectable (n.d.) to 230 ng/m^3 or 326 ng/m^3 for the unassigned and regional class, respectively. The same situation can be observed for PE. Again, PE was mainly found in local samples (n = 7) resulting in a median concentration of 33.3 ng/m^3 (maximum: 195 ng/m^3). Most of the samples of the unassigned and the regional class again showed concentrations below the limit of detection, but maximum values reach up to 221 ng/m^3 (unassigned class) and 290 ng/m^3 (regional class). For both, PP and PE, we could not detect a statistical difference among classes using one-way ANOVA. The few elevated concentrations of PP and PE in samples reflecting the class 'regional' were predominantly determined during March. The investigation of this three month period indicates that PE and PP could be closer linked to local sources, while PET is present most of the time.

Considering UFMNP median concentrations were 136 ng/m^3 (local), 170 ng/m^3 (unassigned) and 228 ng/m^3 (regional) and thus follow the same trend as $PM_{2.5}$ concentrations (see Fig. 2 E). Though, no statistically significant difference between the classes could be observed. The detailed patterns which became visible when evaluating the single polymers are no longer visible, which underlines the importance to investigate the concentrations of single polymers.

3.3. Particle-bound PAH concentrations

In general, total PAH concentrations, hereinafter referred as $\sum_{23}$PAHs, were in the range of 5.25–25.4 ng/m^3, with average concentrations of 13.6 ng/m^3. Table S 3 provides the atmospheric

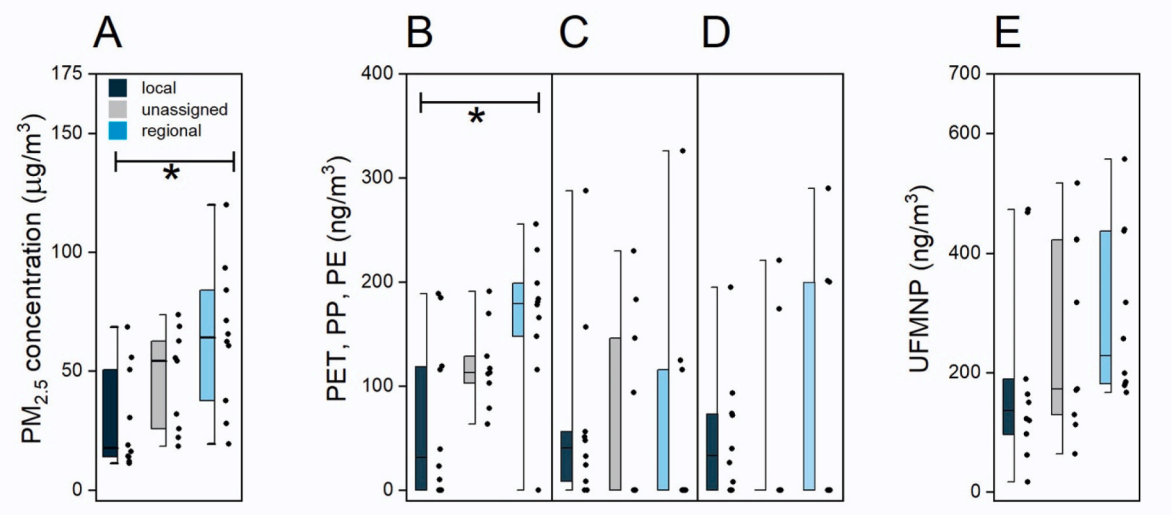

Fig. 2. A-E. (A) Atmospheric $PM_{2.5}$ concentrations grouped according to the three different classes, i.e. local, unassigned and regional. (B–D) Atmospheric PET, PP and PE concentrations for the local, unassigned and regional data sets. (E) Atmospheric UFMNP concentrations for the local, unassigned and regional data sets. Observations of one class are always displayed as boxplot accompanied by the data points itself (black dots). Statistical data analysis was done using one-way ANOVA and differences were considered as significant when p-value <0.05, and are highlighted with '*'.

concentrations for each PAH recorded on a daily basis over the study period. PAH concentrations were rather low during the first days of sampling in January. Lowest PAH contributions were found on the 06.01.2017 ($\sum_{23}$PAH = 5.25 ng/m^3), which was a day accompanied by minimum $PM_{2.5}$ concentrations (11.4 µg/m^3) and lowest concentrations of UFMNP. A seasonal and as such temperature dependent trend of total PAH concentrations is very well known and in accordance with European findings (e.g. Khan et al., 2018; Manoli et al., 2016; Pietrogrande et al., 2022) and mainly caused by changes of emission fluxes (e.g. higher tendency for residential heating due to cold temperatures), but also by the prevailing meteorological conditions favoring temperature inversion. The contribution of PAHs to the overall $PM_{2.5}$ mass were in the sub-‰ range, varying between 0.13 and 0.68‰ and thus clearly lower than UFMNP contributions.

Throughout the study period, highest average PAH contributions can be attributed to BbjkF (2.58 ng/m^3), while lowest average contributions were found for Per (0.18 ng/m^3). Comparisons of the overall PAH concentration with other studies has to be interpreted carefully because most studies do not refer to the same number of PAHs quantified and sometimes also to a different combination of congeners. However, almost all studies quantify BaP, which is a known carcinogen (IARC, 2010) and thus listed as priority compound by the US EPA. BaP concentrations in Graz were in the range of 0.18–2.14 ng/m^3, with peak concentrations observed on 21.01.2017, while lowest BaP concentrations were observed on the 06.01.2017. Average BaP concentrations yield 1.14 ng/m^3 and are higher than those recently reported for other European cities (e.g. Manoli et al., 2016; Pietrogrande et al., 2022), which can be attributed to the fact, that this work focusses on days with marked influence of elevated pollution levels influenced by both, local and regional sources.

The investigation of diagnostic PAH ratios, which are widely used to identify source contributions (e.g. combustion processes, traffic influence) (Tobiszewski et al., 2012), did not present a distinct picture. This can be attributed to the fact, that PM describes the ambient situation and the atmospheric fate of air masses is quite complex (Fleming et al., 2012), while diagnostic ratios are usually derived from emission studies not considering any atmospheric transformations. As the two isomers, BaP and BeP, show differences in their photodegradation, the diagnostic ratio of BaP/(BaP + BeP) can be used to evaluate if particles already underwent atmospheric degradation processes and thus can be reasonably applied to ambient samples too. The BaP/(BaP + BeP) ratio of samples assigned to the regional class yielded a maximum ratio of 0.68, while ratios of samples assigned to the local classed reached higher up (maximum BaP/(BaP + BeP) ratio of 0.95). Findings from emission experiments suggest, that atmospherically degraded particles show BaP/(BaP + BeP) ratios below 0.5 (Tobiszewski et al., 2012), while the diagnostic ratio of freshly emitted ones reaches higher up (Kirchsteiger et al., 2021). Even though extrapolating diagnostic ratios derived from emission experiments to the ambient situation is difficult and has to be interpreted carefully, samples assigned to the local class tend to show higher contributions of fresh emission while samples from the regional and unassigned classes (unassigned: maximum BaP/(BaP + BeP) ratio of 0.64) were already influenced by atmospheric degradation processes.

3.4. Correlations of polymer types with $PM_{2.5}$ mass, OM and EC

Spearman rank coefficients (ρ) were used to investigate the relationship between the polymer types and $PM_{2.5}$ mass as well as PM macro constituents, which may indicate possible co-emission processes, similar transportation pathways or interactions of those compound classes. The correlation analysis refers to the whole dataset, whereas predefined classes are highlighted by differently coloured data points. As the single polymers could not be quantified in every sample, samples yielding zero values were excluded from correlation analysis. Fig. 3 A-F presents the correlations with $PM_{2.5}$, OM and EC showing Spearman rank coefficients ρ > 0.8 and p-values <0.05 which were considered as significantly high monotonic ones. A summary including all correlations is given in the supplement (see Figure S 1 A-L).

PP shows significantly high monotonic correlations (ρ > 0.8) with all macro constituents. For PP the data set refers to a sample size of 15 samples including all classes, though the data set of the regional and unassigned classes is markedly reduced, as several samples showed readings below the detection limit. Highest significant correlations were observed between PP and OM (ρ = 0.97). PE concentrations (n = 12) show significantly high monotonic correlations with $PM_{2.5}$ mass (ρ = 0.89) and OM (ρ = 0.88). EC is also significantly correlated, but yielded a Spearman rank coefficient slightly below 0.8 (ρ = 0.76). Again, the data set for regional and unassigned samples is markedly reduced. In case of PET, the most abundant polymer, the most comprehensive data set could be evaluated. PET showed significant monotonic correlations with all target compounds, i.e. OM (ρ = 0.78) and EC (ρ = 0.53) but only the correlation with the $PM_{2.5}$ mass (ρ = 0.81) exceeded ρ > 0.8, thus

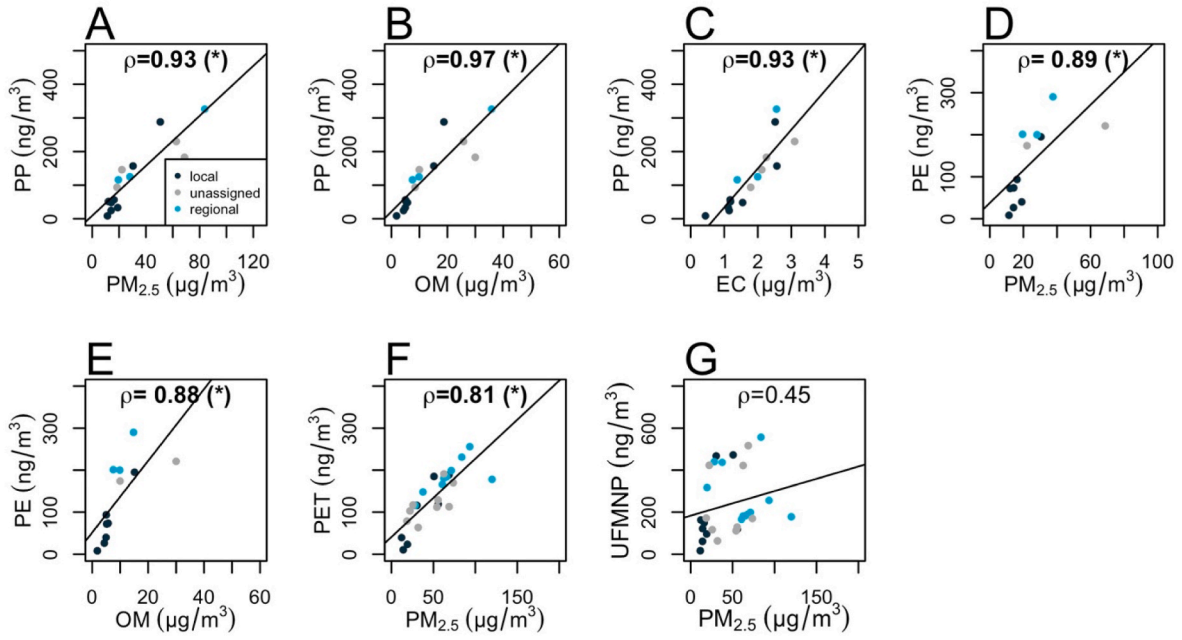

Fig. 3. A-G. Correlations of quantified compounds, i.e. PP, PE and PET and UFMNP with $PM_{2.5}$, OM and EC classified in local (dark blue points), unassigned (grey points) and regional (light blue points) episodes. (*) Highlighted Spearman's rank coefficients mark correlations with a p-value <0.05 were considered as significantly monotonic. All correlations are given in the supplement, Figure S 1 A-L.

being highly correlated. For all polymers it is possible to summarize all data points with one trend line. As soon as the polymer is detectable, the correlations with $PM_{2.5}$, OM or EC are consistent for all samples.

UFMNP showed weak correlations with all target compounds, i.e. $PM_{2.5}$ ($\rho = 0.45$), OM ($\rho = 0.46$). With exception of EC ($\rho = 0.51$), no significant monotonic relationship was found. The data set seems to be separated into two (see Fig. 3 G), which is mainly caused by the fact, that we could not quantify each single polymer in all of the samples, i.e. higher UFMNP concentrations represent samples matching the fingerprints of more than one polymer, while lower concentrations are the samples missing matches for PP and/or PE. These findings highlight the importance of analysing and interpreting individual polymer types and not UFMNP as a bulk compound. Although being all 'plastics' sources, emission fluxes and chemical and physical properties of polymers are different and will lead to different behaviour which might blur the picture when the bulk parameter UFMNP is investigated.

3.5. Correlations of polymer types with individual PAH congeners

The correlation plots between polymers and the individual PAH congeners are given in the supplement (Figure S 2- 5 A-W), while Fig. 4 A-I only highlights correlations considered as significantly high monotonic ($\rho > 0.8$ and p-values <0.05). Among all polymer types, PP concentrations showed the highest number of significant and high monotonic correlations with single PAH congeners. These are found for PP and the highly toxic and carcinogenic high molecular weight (HMW) congeners BaA ($\rho = 0.82$), BeP ($\rho = 0.84$), BghiP ($\rho = 0.90$) and DBaiP ($\rho = 0.90$). Also, PP significantly correlated with two low molecular weight (LMW) PAHs, i.e. Acy ($\rho = 0.82$) and Anthr ($\rho = 0.94$). Again the assignment to sample classes does not affect the correlation between polymer and PAH congener, as long as the polymer is detected. Besides a significant correlation of PE with the LMW congener Anthr ($\rho = 0.89$), PE also highly correlated with three HMW PAHs, i.e. BghiP ($\rho = 0.84$), and two of the dibenzopyrene isomers, i.e. DBaeP ($\rho = 0.83$) and DBaiP ($\rho = 0.81$). Interestingly, we did not find a significant correlation among PE and 135TPB, which has been recently used as a tracer substance for the combustion of PE in atmospheric samples (e.g. Furman et al., 2021; Islam et al., 2020; Simoneit et al., 2005). 135TPB is structurally very different to PAHs as it does not consist of fused benzene rings and thus does not belong to the group of PAHs. We included it in our analyses to get a first impression whether a possible correlation between polymers and PAH congeners could be due to joint emissions during plastic combustion. As no correlation between 135TPB and PE was obtained, a co-emission during combustion seems to be unlikely for our samples. Although PET was the most abundant polymer type, no significant monotonic correlation among PET and any of the PAH congeners could be observed. Even tough, correlation analysis is not sufficient to give evidence of an actual sorption of PAHs with UFMNP, we use this tool to evaluate possible interactions and carrier functions of UFMNP and discuss the results in regard to the available literature. The findings presented in this study agree with previously reported results for aquatic systems, where it was mentioned that PE and PP show higher sorption abilities than other polymers (Fotopoulou et al., 2015; Rochman et al., 2013). Differences in sorption behavior of the individual polymer types may be attributed to their differences in molecular structure. Rubbery polymers such as PE and PP tend to sorb higher amounts of pollutants (Rochman et al., 2013), due to their flexible and expanded structure which is concomitant with a higher accessibility and permeability for partitioning of hydrophobic substances (Wang et al., 2020). Among those two polymer types, PE tends to show a slightly higher sorption capacities of PAHs than observed for PP (Lee et al., 2014). Conversely, glassy polymer types such as PET show lower sorption capacity (Rochman et al., 2013), due to their dense and highly cross-linked structure (Wang et al., 2020). The findings presented in this study are generally in line with previously reported ones, however, we want to point out the main differences among studies, i.e. (i) the present work refers to large palette of PAHs and for most congeners no sorption experiments are available yet, (ii) most sorption experiments investigate either the sorption of PAHs to polymer types or dissolved organic matter (DOM) and this separation of sorbents does not reflect the situation of $PM_{2.5}$ samples as they consist of a variety of chemical species whereas an interplay of different interactions is very likely, and (iii) results obtained from sorption experiments cannot be easily extrapolated to findings presented here as we investigated the relations of polymers and PAHs on the basis of correlations rather than the extraction of PAHs from urban polymer debris, which still presents an technical and analytical

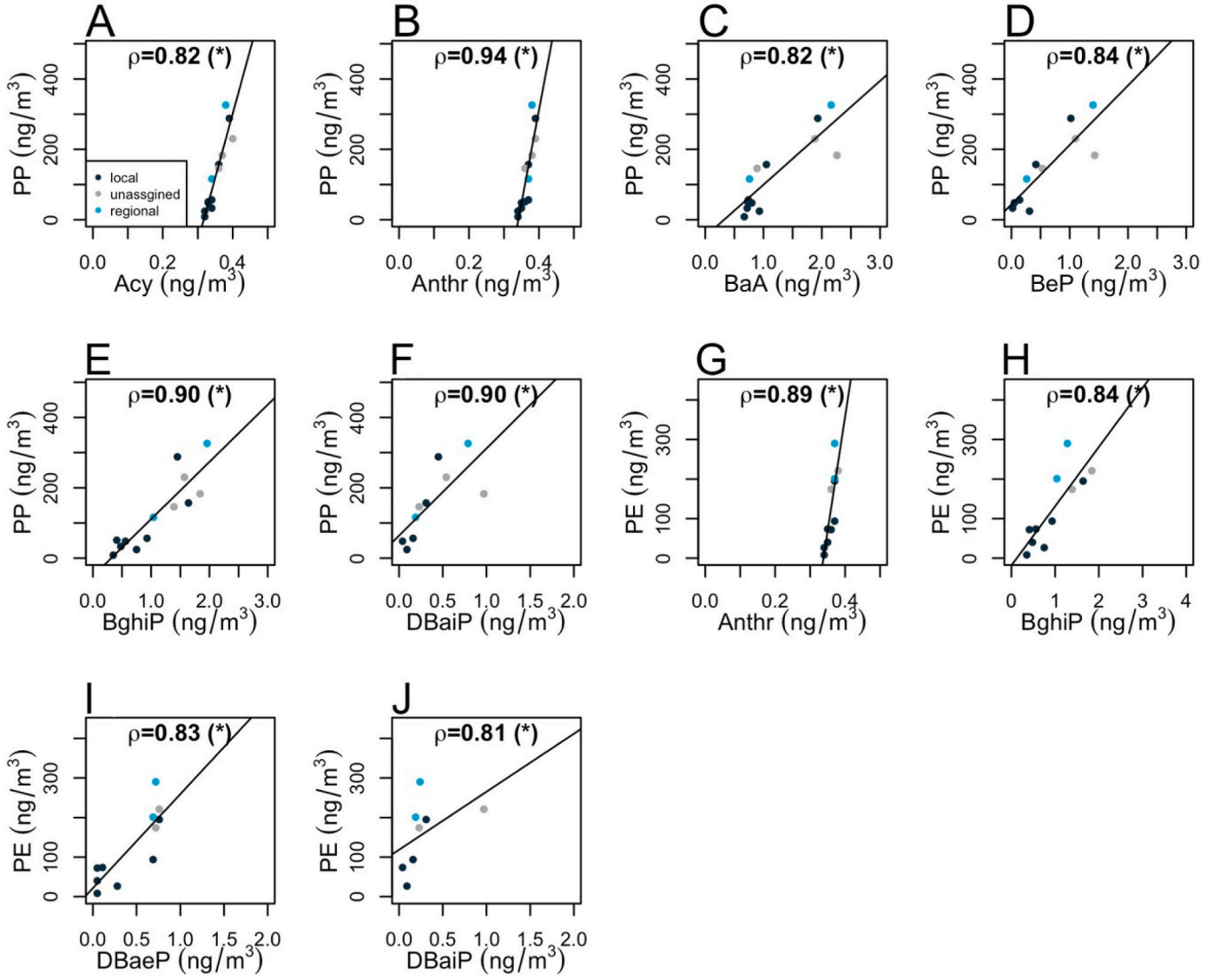

Fig. 4. A-I. Correlations of quantified PP and PE concentrations with those of individual PAH congeners. Note, that this figure only highlights significantly high monotonic correlations with Spearman rank coefficients >0.8 and p-values <0.05. All correlations are given in the supplement, see Figure S 2–5. Sampling days for each assigned class are highlighted in different colors, i.e. local (dark blue points), unassigned (grey points) and regional (light blue points).

challenge. PE and PP showed significantly high monotonic correlations with individual PAH congeners, which gives a first impression about possible interactions. Although further studies are required to elucidate the sort of interaction, i.e. sorption of PAHs to the individual polymers or the co-occurrence of both substance classes in the bulk $PM_{2.5}$.

Grouping PAH congeners according to their molecular weight, i.e. LMW versus HMW PAHs, indicates that correlations are more likely for LMW than for HMW PAHs. We quantified five different LMW PAHs and two of them showed significantly high monotonic relationships with PP and PE, while for HMW PAHs only five out of 18 congeners significantly correlated with the respective polymer types. Also, the correlations given in Fig. 4 for LMW PAHs are more pronounced than the respective correlations between PAHs and OM or EC (see Figure S 6), again pointing to special interactions between UFMNP and organic and toxic pollutants. For HMW PAHs this behavior is less pronounced. Correlations between BaA, BeP, BghiP and DBaiP with EC are similar or even more pronounced compared to the conditions reported in Fig. 4. These findings agree with sorption capacities reported for PAHs and DOM, whereas an increase of sorption capacity with increasing molecular weight of the PAH congener was observed (Kim and Kwon, 2010; Raber et al., 1998). A similar trend can be observed for PAHs and different polymer types (Lee et al., 2014). However, in some cases, sorption capacities observed among the congeners and DOM exhibit higher values than observed for the respective polymer types, e.g. a higher partitioning coefficient was reported for BghiP to humic acids and water (low-$K_{DOC,w} = 7.62 \pm 0.06$) (Kim and Kwon, 2010), than for BghiP to PP and sea water ($logK_{PP,SW} = 6.69$) (Lee et al., 2014). This can be attributed to the higher hydrophobicity of the HMW PAHs interacting with the large hydrophobic backbone and crosslinked aromatic compounds as they are found in humic acids or other polyaromatic species of DOM (Kim and Kwon, 2010). Our results indicate, that polymers possible facilitate the condensation of LMW PAHs that remain preferentially in the gas phase otherwise, while the interaction of HMW PAHs with the polymer types tends to rely on an interplay of different mechanism also involving other polyaromatic constituents of $PM_{2.5}$.

4. Summary and conclusion

The detection of ultrafine microplastics and nanoplastics (UFMNP) in urban particulate matter samples amplifies the palette of

environmental compartments in which plastic particles have been reported. Our results present, for the first time, atmospheric concentrations on the level of single polymer types. By analysing 29 daily $PM_{2.5}$ samples within the time period of 02.01. – 31.03.2017, we were able to quantify atmospheric concentrations of three emerging polymer types, i.e. polyethylene terephthalate (PET), polypropylene (PP) and polyethylene (PE). Among those, PET has been identified as the most prominent polymer type accounting for 50% of the overall UFMNP mass, while polypropylene (PP) and polyethylene (PE) accounted for 27% and 23%, respectively. On average, UFMNP compose 0.67% of the overall $PM_{2.5}$ mass. On the single polymer level, highest concentrations amount for 256 ng/m^3 (PET), 326 ng/m^3 (PP) and 290 ng/m^3 (PE). These findings clearly highlighting the emerging role of polymer compounds in atmospheric samples.

To investigate a potential ability of polymers in particulate matter samples to adsorb PAHs we additionally quantified the atmospheric concentrations of 23 individual PAH congeners. Overall PAH concentrations were on average 13.6 ng/m^3. We identified significantly high monotonic correlations of PP and PE with single PAH congeners including highly toxic and carcinogenic ones (i.e. Acy, Anthr, BaA, BeP, BghiP, DBaeP and DBaiP). Although PET was the most abundant polymer type, no significantly high correlation was found among PAH congeners. These findings agree with results obtained from sorption experiments in aqueous systems, where higher abilities for PAH adsorption were found for PP and PE, than for other polymer types. It appears that correlations are more likely among LMW PAHs and polymer types than observed for HMW PAHs, indicating possible carrier activities of UFMNP for LMW PAHs. The present work is the first one discussing relationships of polymer compounds and PAHs found in urban particulate matter samples and highlights the importance of further studies to improve the understanding of polymers as PAH vehicles for atmospheric transport and the potential health outcomes.

CRediT authorship contribution statement

Bernadette Kirchsteiger: Conceptualization, Methodology, Formal analysis, Investigation, Writing – original draft, Writing – review & editing, Visualization. **Dušan Materić:** Conceptualization, Resources, Methodology, Data curation, Writing – original draft, Writing – review & editing, Visualization. **Felix Happenhofer:** Investigation, Writing – review & editing. **Rupert Holzinger:** Resources, Software, Writing – review & editing. **Anne Kasper-Giebl:** Conceptualization, Resources, Writing – review & editing.

Declaration of competing interest

The authors declare that they have no known competing financial interests or personal relationships that could have appeared to influence the work reported in this paper.

Data availability

All data needed to evaluate the conclusions in the paper (including raw files, the scripts and processing stages of the data analysis) are available at https://doi.org/10.24416/UU01-HKNCGC.

Acknowledgments

The authors gratefully acknowledge the provincial government of Styria (Austria) for providing the filter material. The authors also acknowledge the support from Dutch Research Council (Nederlandse Organisatie Voor Wetenschappelijk Onderzoek –NWO) projects: "Nanoplastics: hormone-mimicking and inflammatory responses?" (grant number OCENW.XS2.078) and "Size distribution of nanoplastics in indoor, urban and rural air" (grant number OCENW.XS21.2.042) provided to Dušan Materić. Two research stays of Bernadette Kirchsteiger at IMAU Utrecht, Utrecht University were financed by the Christiana Hörbiger scholarschip 2019 and the LIONS sponsorship 2021.

Appendix A. Supplementary data

Supplementary data to this article can be found online at https://doi.org/10.1016/j.atmosenv.2023.119670.

References

Akhbarizadeh, R., Dobaradaran, S., Amouei Torkmahalleh, M., et al., 2021. Suspended fine particulate matter (PM2.5), microplastics (MPs), and polycyclic aromatic hydrocarbons (PAHs) in air: their possible relationships and health implications. Environ. Res. 192, 110339 https://doi.org/10.1016/j.envres.2020.110339.

Allen, S., Allen, D., Phoenix, V.R., et al., 2019. Atmospheric transport and deposition of microplastics in a remote mountain catchment. Nat. Geosci. 12 (5), 339–344. https://doi.org/10.1038/s41561-019-0335-5.

Allen, S., Materić, D., Allen, D., et al., 2022. An early comparison of nano to microplastic mass in a remote catchment's atmospheric deposition. Journal of Hazardous Materials Advances 7. https://doi.org/10.1016/j.hazadv.2022.100104.

Avio, C.G., Gorbi, S., Regoli, F., 2017. Plastics and microplastics in the oceans: from emerging pollutants to emerged threat. Mar. Environ. Res. 128, 2–11. https://doi.org/10.1016/j.marenvres.2016.05.012.

Bergmann, M., Collard, F., Fabres, J., et al., 2022. Plastic pollution in the arctic. Nat. Rev. Earth Environ. https://doi.org/10.1038/s43017-022-00279-8.

Cai, L., Wang, J., Peng, J., et al., 2017. Characteristic of microplastics in the atmospheric fallout from Dongguan city, China: preliminary research and first evidence. Environ. Sci. Pollut. Res. Int. 24 (32), 24928–24935. https://doi.org/10.1007/s11356-017-0116-x.

Cavalli, F., Viana, M., Yttri, K.E., et al., 2010. Toward a standardised thermal- optical protocol for measuring atmospheric organic and elemental carbon: the EUSAAR protocol. Atmos. Meas. Tech. 3 (1), 79–89. https://doi.org/10.5194/amt-3-79-2010.

Corradini, F., Meza, P., Eguiluz, R., et al., 2019. Evidence of microplastic accumulation in agricultural soils from sewage sludge disposal. Sci. Total Environ. 671, 411–420. https://doi.org/10.1016/j.scitotenv.2019.03.368.

Dris, R., Gasperi, J., Saad, M., et al., 2016. Synthetic fibers in atmospheric fallout: a source of microplastics in the environment? Mar. Pollut. Bull. 104 (1–2), 290–293. https://doi.org/10.1016/j.marpolbul.2016.01.006.

EEA, 2019. Air Quality in Europe - 2019 Report. https://doi.org/10.2800/777411.

EN 12341, 2014. EN 12341:2014-08, Ambient Air - Standard Gravimetric Measurement Method for the Determination of PM10 or PM2.5 Mass Concentration of Suspended Particulate Matter. Brussels, European Comittee for Standardization, p. p 62.

EN 15549, 2008. EN 15549:2008-06, Air Quality - Standard Method for the Measurement of the Concentration of Benzo(a)pyrene in Ambient Air. Brussels, European Committee for Standardization, p. p 53.

EN 16450, 2017. In: EN 16450:2017, Ambient Air - Automated Measuring Systems for the Measurement of the Concentration of Particulate Matter. Brussels, European Committee for Standardization. PM10, PM2.5.

EN 16909, 2017. EN 16909:2017-06, Ambient air - measurement of elemental carbon (EC) and organic carbon (OC) collected on filter. In: E.C.f. (Ed.), Standardization. Brussels, European Comittee for Standardization.

Fleming, Z.L., Monks, P.S., Manning, A.J., 2012. Review: untangling the influence of air-mass history in interpreting observed atmospheric composition. Atmos. Res. 104–105, 1–39. https://doi.org/10.1016/j.atmosres.2011.09.009.

Fotopoulou, K.N., Karapanagioti, H.K., 2015. Surface properties of beached plastics. Environ. Sci. Pollut. Res. Int. 22 (14), 11022–11032. https://doi.org/10.1007/s11356-015-4332-y.

Furman, P., Styszko, K., Skiba, A., et al., 2021. Seasonal variability of PM10 chemical composition including 1,3,5-triphenylbenzene, marker of plastic combustion and toxicity in Wadowice, South Poland. Aerosol Air Qual. Res. 21, 3. https://doi.org/10.4209/aaqr.2020.05.0223.

Gasperi, J., Wright, S.L., Dris, R., et al., 2018. Microplastics in air: are we breathing it in? Curr. Opin. in Environ. Sci. Health 1, 1–5. https://doi.org/10.1016/j.coesh.2017.10.002.

Hirai, H., Takada, H., Ogata, Y., et al., 2011. Organic micropollutants in marine plastics debris from the open ocean and remote and urban beaches. Mar. Pollut. Bull. 62 (8), 1683–1692. https://doi.org/10.1016/j.marpolbul.2011.06.004.

Holzinger, R., 2015. PTRwid: a new widget tool for processing PTR-TOF-MS data. Atmos. Meas. Tech. 8 (9), 3903–3922. https://doi.org/10.5194/amt-8-3903-2015.

IARC, 2010. Some Non-heterocyclic Polycyclic Aromatic Hydrocarbons and Some Related Exposures in IARC Monographs on the Evaluation of Carcinogenic Risk to Humans.

Islam, M.R., Jayarathne, T., Simpson, I.J., et al., 2020. Ambient air quality in the Kathmandu Valley, Nepal, during the pre-monsoon: concentrations and sources of particulate matter and trace gases. Atmos. Chem. Phys. 20 (5), 2927–2951. https://doi.org/10.5194/acp-20-2927-2020.

Khan, M., Masiol, M., Bruno, C., et al., 2018. Potential sources and meteorological factors affecting PM 2.5 -bound polycyclic aromatic hydrocarbon levels in six main cities of northeastern Italy: an assessment of the related carcinogenic and mutagenic risks. Environ. Sci. Pollut. Control Ser. 25 (32), 31987–32000. https://doi.org/10.1007/s11356-018-2841-1.

Kim, S.-J., Kwon, J.-H., 2010. Determination of partition coefficients for selected PAHs between water and dissolved organic matter. CLEAN - Soil, Air, Water 38 (9), 797–802. https://doi.org/10.1002/clen.201000113.

Kirchsteiger, B., Kistler, M., Steinkogler, T., et al., 2020. Combination of different approaches to infer local or regional contributions to PM2.5 burdens in Graz, Austria. Appl. Sci. 10, 12. https://doi.org/10.3390/app10124222.

Kirchsteiger, B., Kubik, F., Sturmlechner, R., et al., 2021. Real-life emissions from residential wood combustion in Austria: from TSP emissions to PAH emission profiles, diagnostic ratios and toxic risk assessment. Atmos. Pollut. Res. 12 (8) https://doi.org/10.1016/j.apr.2021.101127.

Klein, M., Fischer, E.K., 2019. Microplastic abundance in atmospheric deposition within the Metropolitan area of Hamburg, Germany. Sci. Total Environ. 685, 96–103. https://doi.org/10.1016/j.scitotenv.2019.05.405.

Lee, H., Shim, W.J., Kwon, J.H., 2014. Sorption capacity of plastic debris for hydrophobic organic chemicals. Sci. Total Environ. 470–471, 1545–1552. https://doi.org/10.1016/j.scitotenv.2013.08.023.

Lenschow, P., Abraham, H.J., Kutzner, K., et al., 2001. Some ideas about the sources of PM10. Atmos. Environ. 35, S23–S33. https://doi.org/10.1016/S1352-2310(01)00122-4.

Mai, L., He, H., Bao, L.J., et al., 2020. Plastics are an insignificant carrier of riverine organic pollutants to the Coastal oceans. Environ. Sci. Technol. 54 (24), 15852–15860. https://doi.org/10.1021/acs.est.0c05446.

Manoli, E., Kouras, A., Karagkiozidou, O., et al., 2016. Polycyclic aromatic hydrocarbons (PAHs) at traffic and urban background sites of northern Greece: source apportionment of ambient PAH levels and PAH-induced lung cancer risk. Environ. Sci. Pollut. Control Ser. 23 (4), 3556–3568. https://doi.org/10.1007/s11356-015-5573-5.

Materić, D., Kasper-Giebl, A., Kau, D., et al., 2020. Micro- and nanoplastics in alpine snow: a new method for chemical identification and (Semi)Quantification in the Nanogram range. Environ. Sci. Technol. 54 (4), 2353–2359. https://doi.org/10.1021/acs.est.9b07540.

Materić, D., Kjaer, H.A., Vallelonga, P., et al., 2022a. Nanoplastics measurements in Northern and Southern polar ice. Environ. Res. 208, 112741 https://doi.org/10.1016/j.envres.2022.112741.

Materić, D., Ludewig, E., Brunner, D., et al., 2021. Nanoplastics transport to the remote, high-altitude Alps. Environ. Pollut. 288, 117697 https://doi.org/10.1016/j.envpol.2021.117697.

Materić, D., Peacock, M., Dean, J., et al., 2022b. Presence of nanoplastics in rural and remote surface waters. Environ. Res. Lett. https://doi.org/10.1088/1748-9326/ac68f7.

Pietrogrande, M.C., Bacco, D., Demaria, G., et al., 2022. Polycyclic aromatic hydrocarbons and their oxygenated derivatives in urban aerosol: levels, chemical profiles, and contribution to PM2.5 oxidative potential. Environ. Sci. Pollut. Res. Int. https://doi.org/10.1007/s11356-021-16858-z.

Plastics Europe, 2021. In: Europe, P. (Ed.), Plastics - the Facts 2021, an Analysis of European Plastics Production, Demand and Waste Data, Belgium, Plastics Europe.

Raber, B., Kögel-Knabner, I., Stein, C., et al., 1998. Partitioning of polycyclic aromatic hydrocarbons to dissolved organic matter from different soils. Chemosphere 36 (1), 79–97. https://doi.org/10.1016/S0045-6535(97)00352-4.

Rochman, C.M., Hoh, E., Hentschel, B.T., et al., 2013. Long-term field measurement of sorption of organic contaminants to five types of plastic pellets: implications for plastic marine debris. Environ. Sci. Technol. 47 (3), 1646–1654. https://doi.org/10.1021/es303700s.

Seidensticker, S., Zarfl, C., Cirpka, O.A., et al., 2017. Shift in mass transfer of Wastewater contaminants from microplastics in the presence of dissolved substances. Environ. Sci. Technol. 51 (21), 12254–12263. https://doi.org/10.1021/acs.est.7b02664.

Simoneit, B.R.T., Medeiros, P.M., M, D.B., 2005. Combustion products of plastics as indicators for refuse burning in the atmosphere. Environ. Sci. Technol. 39, 6961–6970. https://doi.org/10.1021/es050767x.

Sridharan, S., Kumar, M., Singh, L., et al., 2021. Microplastics as an emerging source of particulate air pollution: a critical review. J. Hazard Mater. 418, 126245 https://doi.org/10.1016/j.jhazmat.2021.126245.

Tobiszewski, M., Namiesnik, J., 2012. PAH diagnostic ratios for the identification of pollution emission sources. Environ. Pollut. 162, 110–119. https://doi.org/10.1016/j.envpol.2011.10.025.

Torres, F.G., Dioses-Salinas, D.C., Pizarro-Ortega, C.I., et al., 2021. Sorption of chemical contaminants on degradable and non-degradable microplastics: recent progress and research trends. Sci. Total Environ. 757, 143875 https://doi.org/10.1016/j.scitotenv.2020.143875.

Wang, T., Wang, L., Chen, Q., et al., 2020. Interactions between microplastics and organic pollutants: effects on toxicity, bioaccumulation, degradation, and transport. Sci. Total Environ. 748, 142427 https://doi.org/10.1016/j.scitotenv.2020.142427.

Wang, W., Wang, J., 2018. Comparative evaluation of sorption kinetics and isotherms of pyrene onto microplastics. Chemosphere 193, 567–573. https://doi.org/10.1016/j.chemosphere.2017.11.078.

Wright, S.L., Ulke, J., Font, A., et al., 2020. Atmospheric microplastic deposition in an urban environment and an evaluation of transport. Environ. Int. 136, 105411 https://doi.org/10.1016/j.envint.2019.105411.